

## Correlations of Synthetic, Spectroscopic, Structural, and Speciation Studies in the Biologically Relevant Cobalt(II)–Citrate System: The Tale of the First Aqueous Dinuclear Cobalt(II)–Citrate Complex

N. Kotsakis,<sup>†</sup> C. P. Raptopoulou,<sup>‡</sup> V. Tangoulis,<sup>§</sup> A. Terzis,<sup>‡</sup> J. Giapintzakis,<sup>||</sup> T. Jakusch,<sup>⊥</sup> T. Kiss,<sup>⊥</sup> and A. Salifoglou<sup>\*†</sup>

Department of Chemistry, University of Crete, Heraklion 71409, Greece, Institute of Materials Science, NCSR “Demokritos”, Aghia Paraskevi 15310, Attiki, Greece, Department of Materials Science, University of Patras, 26500 Patras, Greece, Institute of Electronic Structure and Laser, FORTH, 71110 Heraklion, Greece, and Department of Inorganic and Analytical Chemistry, Biocoordination Chemistry Research Group of the Hungarian Academy of Sciences, University of Szeged, Szeged, H-6720 Hungary

Received December 11, 2001

Synthetic efforts targeting soluble species of Co(II) with the low molecular mass physiological ligand citric acid led to the isolation of the first dinuclear complex  $[\text{Co}_2(\text{C}_6\text{H}_5\text{O}_7)_2(\text{H}_2\text{O})_4]^{2-}$ , at pH  $\sim 5$ , in the form of its  $\text{K}^+$  (**1**) and  $\text{Na}^+$  (**2**) salts. Both **1** and **2** were characterized analytically, spectroscopically (FT-IR, UV/visible, EPR), and magnetically. Complex **1** crystallizes in the monoclinic space group  $P2_1/n$ , with  $a = 10.348(5)$  Å,  $b = 11.578(6)$  Å,  $c = 12.138(6)$  Å,  $\beta = 112.62(2)^\circ$ ,  $V = 1342(1)$  Å<sup>3</sup>, and  $Z = 2$ . Complex **2** crystallizes in the monoclinic space group  $P2_1/c$ , with  $a = 9.234(4)$  Å,  $b = 11.913(4)$  Å,  $c = 11.728(6)$  Å,  $\beta = 99.93(2)^\circ$ ,  $V = 1271(1)$  Å<sup>3</sup>, and  $Z = 2$ . X-ray crystallography on **1** and **2** reveals the presence of two Co(II) ions, in a dinuclear assembly, octahedrally coordinated by two citrate ligands in a tridentate fashion. The octahedral environment around each Co(II) is complemented by another singly bonded citrate belonging to the adjacent Co(II) unit and two water molecules. Magnetic susceptibility and EPR studies on **1**, in the solid state, corroborate the X-ray results, indicating a weak interaction between the two Co(II) ions. Moreover, EPR and UV/visible studies in solution suggest that **1** does not retain its dimeric structure, yielding a mononuclear octahedral Co(II)–citrate species. Detailed speciation studies suggest the presence of a number of species including the mononuclear complex  $[\text{Co}(\text{C}_6\text{H}_5\text{O}_7)]^-$ , optimally present around pH  $\sim 5$ . In consonance with EPR and UV/visible spectroscopy,  $[\text{Co}(\text{C}_6\text{H}_5\text{O}_7)]^-$  is likely the scaffolding unit on the basis of which the dimer  $[\text{Co}_2(\text{C}_6\text{H}_5\text{O}_7)_2(\text{H}_2\text{O})_4]^{2-}$  is isolated from aqueous solutions. Collectively, this comprehensive study offers significant structural insight into the Co(II)–citrate speciation and the elucidation of the role of Co(II) in biological fluids.

### Introduction

Citric acid has been widely known for its abundance in physiological fluids and its multipotent chemical versatility toward biologically relevant metal ions.<sup>1,2</sup> It actively participates in the Krebs cycle<sup>3,4</sup> and is an essential component in a number of metalloenzyme active sites, including the

NifV<sup>-</sup> nitrogenase cofactor<sup>5–7</sup> and the aconitase iron–sulfur cluster.<sup>8</sup> More importantly, though, it presents a chemically attractive ligand target to a number of trace metal ions circulating in biological fluids, including those in humans. Complexation to such metal ions begets solubility, potential

\* To whom correspondence should be addressed. Tel: +30-281-0393-652. Fax: +30-281-0393-601. E-mail: salif@chemistry.uoc.gr.

<sup>†</sup> University of Crete.

<sup>‡</sup> NCSR “Demokritos”. E-mail: craptop@ims.ariadne-t.gr.

<sup>§</sup> University of Patras. E-mail: vtango@upatras.gr.

<sup>||</sup> FORTH. E-mail: giapintz@iesl.forth.gr.

<sup>⊥</sup> University of Szeged. E-mail: tkiss@chem.u-szeged.hu.

(1) Srere, P. A. *Curr. Top. Cell. Regul.* **1972**, *5*, 229–283.

(2) Glusker, J. P. *Acc. Chem. Res.* **1980**, *13*, 345–352.

(3) Krebs, H. A.; Johnson, W. A. *Enzymologia* **1937**, *4*, 148–156.

(4) Crans, D. C. In *Metal Ions in Biological Systems: Vanadium and its Role in Life*; Sigel, H., Sigel, A. E., Eds.; Marcel Dekker: New York, 1995; Chapter 5, pp 147–209.

(5) Beinert, H. *FASEB J.* **1990**, *4*, 2483–2491.

(6) Beinert, H.; Kennedy, M. C. *Eur. J. Biochem.* **1989**, *186*, 5–15.

(7) Lippard, S. J.; Berg, J. M. In *Principles of Bioinorganic Chemistry*; University Science Books: Mill Valley, CA, 1994; Chapter 12, pp 352–354.

(8) Eady, R. R. In *Metal Ions in Biological Systems: Vanadium and its Role in Life*; Sigel, H., Sigel, A., Eds.; Marcel Dekker, Inc.: New York, NY, 1995; Vol. 31, Chapter 11, pp 363–405.

bioavailability, and likely absorption to biological sites in need of those essential metals. Cobalt is one of those trace metals, which is present in the human body, as a metal cofactor, in the form of biologically important molecules, like the B<sub>12</sub> coenzyme and vitamin B<sub>12</sub>.<sup>9–12</sup> Cobalt has also been known for its potent influence on human pathophysiological conditions resulting either from (a) its absence in the body, thereby leading to anemic symptomatology<sup>13</sup> or (b) its presence in excess, emerging from professional or habitual exposure, leading to toxic effects manifested in heart disease and excessive red corpuscle formation.<sup>14,15</sup> The forms, however, with which low molecular mass physiological ligands, like citrate, complex cobalt ions, thus affording soluble and potentially available species to biochemical processes, are not well-known and even less well structurally characterized. Moreover, knowledge of cobalt speciation patterns with physiological ligands is essential in understanding the role of that metal ion in processes which either support normal biological functions or impart aberrations to human physiology. The paucity of structural information on various cobalt(II)–citrate species has prompted us to investigate in depth the solution behavior of such a binary system and attempt to identify the species involved in the related aqueous biodistribution patterns. As a first token of that effort, we had previously reported on the first structurally characterized mononuclear complex (NH<sub>4</sub>)<sub>4</sub>[Co(C<sub>6</sub>H<sub>5</sub>O<sub>7</sub>)<sub>2</sub>].<sup>16</sup> Herein, we report synthetic, spectroscopic, magnetic, and structural studies on the first dinuclear Co(II)–citrate complex and correlate its behavior in the solid state and in solution with that of species arising from solution speciation studies on the Co(II)–citrate system.

## Materials and Methods

Manipulations were carried out in the open air. Since Co(II), however, is sensitive to oxidation to the inert Co(III) form in basic media, potentiometric titrations, which were extended up to pH ~11, were carried out under an argon atmosphere. Co(NO<sub>3</sub>)<sub>2</sub>·6H<sub>2</sub>O, CoCl<sub>2</sub>·6H<sub>2</sub>O, and anhydrous citric acid were purchased from Fluka. KOH and NaOH were purchased from Aldrich. Nano-pure quality water was used for all reactions run. The quality of the chemicals employed in the speciation studies was the best available. The purity of citric acid and other reagents, and whenever possible the exact concentration of their solutions (prepared freshly every day), were determined by the Gran method.<sup>17–19</sup> The Co(II) stock solution was

prepared from recrystallized CoCl<sub>2</sub>·6H<sub>2</sub>O. The ionic strength of all the solutions was adjusted to 0.2 M with KCl. In all potentiometric experiments carried out, the temperature remained constant at 25.0 ± 0.1 °C.

**Preparations. K<sub>2</sub>[Co<sub>2</sub>(C<sub>6</sub>H<sub>5</sub>O<sub>7</sub>)<sub>2</sub>(H<sub>2</sub>O)<sub>4</sub>]·6H<sub>2</sub>O (1).** A 2.90 g (9.96 mmol) amount of Co(NO<sub>3</sub>)<sub>2</sub>·6H<sub>2</sub>O was dissolved in 15 mL of nano-pure water. To that solution, 2.00 g (10.4 mmol) of anhydrous citric acid was added under continuous stirring. The pH of the resulting solution was raised to ~5 with 0.1 M KOH. Subsequently, the reaction mixture was stirred overnight at 50 °C. On the following day, the solution was taken to dryness with a rotary evaporator. The produced solid was redissolved in water, under mild heating. Slow evaporation of this solution yielded a pink crystalline material after a few days. The pink crystals were isolated by filtration and dried in vacuo. Yield: 2.15 g (57.1%). Anal. Calcd for C<sub>12</sub>H<sub>30</sub>O<sub>24</sub>K<sub>2</sub>Co<sub>2</sub> (MW 754.42): C, 19.09; H, 3.98; K, 10.33. Found: C, 19.62; H, 4.01; K, 10.54.

**Na<sub>2</sub>[Co<sub>2</sub>(C<sub>6</sub>H<sub>5</sub>O<sub>7</sub>)<sub>2</sub>(H<sub>2</sub>O)<sub>4</sub>]·6H<sub>2</sub>O (2). Method 1.** A 2.90 g (9.96 mmol) amount of Co(NO<sub>3</sub>)<sub>2</sub>·6H<sub>2</sub>O and 2.00 g (10.4 mmol) of anhydrous citric acid were dissolved in 15 mL of water under continuous stirring. The pH of the resulting solution was raised to ~5 with 0.1 M NaOH. Subsequently, the reaction mixture was stirred overnight at 50 °C. On the following day, the solution was taken to dryness with a rotary evaporator. The produced solid was redissolved in a water/ethanol mixture 8:1 (v/v), under mild heating. The derived reaction mixture was allowed to slowly evaporate at room temperature. A few days later, a pink crystalline material appeared at the bottom of the flask. The pink crystals were isolated by filtration and dried in vacuo. Yield: 1.78 g (49.4%). Anal. Calcd for C<sub>12</sub>H<sub>30</sub>O<sub>24</sub>Na<sub>2</sub>Co<sub>2</sub> (MW 722.20): C, 19.93; H, 4.15; Na, 6.37. Found: C, 20.01; H, 4.24; Na, 6.42.

**Method 2.** A 0.16 g (0.55 mmol) amount of Co(NO<sub>3</sub>)<sub>2</sub>·6H<sub>2</sub>O and 0.21 g (1.1 mmol) of anhydrous citric acid were dissolved in water under continuous stirring. The resulting reaction mixture was stirred overnight at 50 °C. On the following day, the solution was taken to dryness with a rotary evaporator. The produced residue was redissolved in 3 mL of water, and the pH of the new solution was raised to ~5 with 0.1 M NaOH. Addition of ethanol to the reaction solution, at 4 °C, yielded a few days later a pink crystalline material at the bottom of the flask. The pink crystals were isolated by filtration and dried in vacuo. Yield: 0.12 g (60%). Positive identification of the pink crystalline material was achieved with the aid of FT-infrared spectroscopy and the X-ray unit cell determination of a single crystal.

**Physical Measurements.** Electronic spectra were recorded in water on a Hitachi U-2001 and a Perkin-Elmer Lambda 2S UV/visible spectrophotometer in the range 200–1000 nm. FT-infrared measurements were taken on a Perkin-Elmer 1760X FT-IR spectrometer. The EPR spectra of complex **1** in the solid state and in solution were recorded on a Bruker ER 200D-SRC X-band spectrometer, equipped with an Oxford ESR 9 cryostat at 9.174 GHz and 10dB and in the temperature range 4–40 K. Magnetic susceptibility data were collected on powdered samples of **1** with a Quantum Design SQUID susceptometer in the 1.9–290 K temperature range. Elemental analyses were performed by Quantitative Technologies, Inc.

**Potentiometric Measurements.** The stability constants of the proton and Co(II) complexes of citric acid (H<sub>3</sub>L<sup>0</sup> = C<sub>6</sub>H<sub>8</sub>O<sub>7</sub>) were determined by pH-metric measurements. Specifically, titrations were carried out on 10 mL samples. The concentration of the citric acid

- (9) Taylor, D. M.; Williams, D. R. In *Trace Element Medicine and Chelation Therapy*; The Royal Society of Chemistry: Cambridge, U.K., 1995.
- (10) Balachandran, S.; Vishwakarma, R. A.; Monaghan, S. M.; Prella, A.; Stamford, N. P. J.; Leeper, F. J.; Battersby, A. R. *J. Chem. Soc., Perkin Trans.* **1994**, 1, 487–491.
- (11) Battersby, A. R. *Acc. Chem. Res.* **1993**, 26, 15–21.
- (12) Debussche, L.; Couder, M.; Thibaut, D.; Cameron, B.; Crouzet, J.; Blanche, F. *J. Bacteriol.* **1992**, 22, 7445–7451.
- (13) Hamilton, E. M. N.; Gropper, S. A. S. In *The Biochemistry of Human Nutrition*; West Publ. Co.: New York, 1987; pp 298–301.
- (14) Helis, H. M.; de Meester, P.; Hodgson, D. J. *J. Am. Chem. Soc.* **1976**, 99, 3309–3312.
- (15) Waldbott, G. L. In *Health Effects of Environmental Pollutants*; C. V. Mosby Co.: St. Louis, MO, 1973.
- (16) Matzapetakis, M.; Dakanali, M.; Raptopoulou, C. P.; Tangoulis, V.; Terzis, A.; Giapintzakis, J.; Salifoglou, A. *J. Biol. Inorg. Chem.* **2000**, 5, 469–474.
- (17) Gran, G. *Acta Chem. Scand.* **1950**, 29, 559.

(18) Gran, G. *Analyst* **1952**, 77, 661–671.

(19) Rossotti, F. J. C.; Rossotti, H. J. *Chem. Educ.* **1965**, 42, 375–378.

solution was in the range 0.002–0.004 M, and the employed metal-to-ligand ratios were 1:2, 2:2, 2:4, 4:4, and 1:4. For the 1:2 and 2:2 titrations, the concentration of citric acid was 0.002 M, while in the rest of the titrations the concentration of citric acid was 0.004 M. The titrations were carried out in the pH range 2–11, with a carbonate-free KOH solution of known concentration (ca. 0.2 M), under a purified argon atmosphere. Duplicate titrations were performed, and the reproducibility of the titration curves was within 0.005 pH units throughout the whole pH range. The pH measurements were made with a Radiometer PHM 84 instrument, using a CMAWL Russel combined glass electrode, which was calibrated for  $[H^+]$  ion concentration according to Irving et al.<sup>20</sup> The ionic product of water was found to be  $pK_w = 13.76$ . Concentration stability constants ( $\beta_{pqr} = [M_pL_qH_r]/[M]^p[L]^q[H]^r$ ) for the proton and Co(II)–citrate complexes formed in the investigated systems were calculated with the general computational program PSEQUAD.<sup>21</sup>

#### Data Collection and X-ray Crystal Structure Determination.

Single crystals of complexes **1** and **2** were obtained from aqueous solutions according to the described synthetic procedures. A single crystal with approximate dimensions 0.10 × 0.20 × 0.50 mm for **1**, and 0.05 × 0.20 × 0.22 mm for **2**, was mounted on a capillary. Diffraction measurements were taken on a Crystal Logic dual-goniometer diffractometer, using graphite monochromated Mo K $\alpha$  radiation. Unit cell dimensions for **1** and **2** were determined and refined by using the angular settings of 25 automatically centered reflections in the range  $11 < 2\theta < 23^\circ$ . Intensity data for both crystals were recorded using  $\theta$ – $2\theta$  scans. Further experimental crystallographic details: for **1**,  $2\theta_{max} = 50^\circ$ , scan speed  $3.0^\circ/\text{min}$ , scan range  $2.3 + \alpha_1\alpha_2$  separation, reflections collected/unique/used 2472/2357 [ $R_{int} = 0.0320$ ]/2357, 241 parameters refined,  $(\Delta/\sigma)_{max} = 0.006$ ,  $(\Delta\rho)_{max}/(\Delta\rho)_{min} = 0.780/-0.570 \text{ e}/\text{\AA}^3$ ,  $R/R_w$  (for all data) 0.0385/0.0898; for **2**,  $2\theta_{max} = 50^\circ$ , scan speed  $2.0^\circ/\text{min}$ , scan range  $2.3 + \alpha_1\alpha_2$  separation, reflections collected/unique/used 2341/2224 ( $R_{int} = 0.0134$ )/2224, 241 parameters refined,  $(\Delta/\sigma)_{max} = 0.003$ ,  $(\Delta\rho)_{max}/(\Delta\rho)_{min} = 0.629/-0.693 \text{ e}/\text{\AA}^3$ ,  $R/R_w$  (for all data) 0.0343/0.0833. A summary of crystallographic data for **1** and **2** is given in Table 1.

Three standard reflections were monitored every 97 reflections over the course of data collection and showed less than 3% variation and no decay. For **1** and **2**, Lorentz, polarization, and  $\psi$ -scan absorption corrections were applied by using Crystal Logic software. The structures of **1** and **2** were solved by direct methods using SHELXS-86<sup>22</sup> and refined by full-matrix least-squares techniques on  $F^2$  with SHELXL-97.<sup>23</sup> All hydrogen atoms in **1** and **2** were located by difference maps and refined isotropically. All non-hydrogen atoms in **1** and **2** were refined anisotropically.

## Results

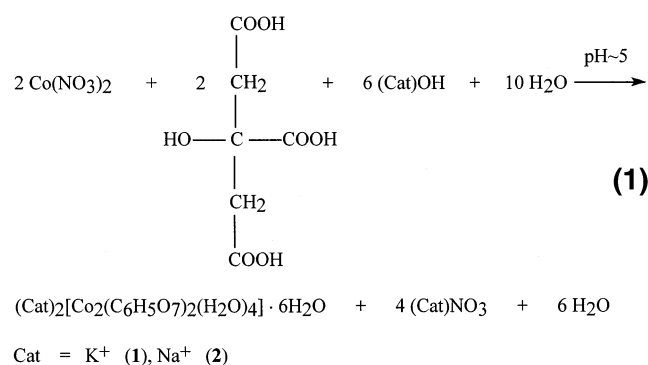
**Syntheses.** In an expedient synthetic procedure, cobalt(II) nitrate and anhydrous citric acid reacted in water with molar ratios ranging from 1:1 to 1:2 at pH  $\sim$ 5 (reaction 1). The bases used for these syntheses, KOH for complex **1** and NaOH for complex **2**, were essential for the reaction. In fact, they raised the pH of the reaction mixture to the desired value, thus contributing to the deprotonation of the citrate

**Table 1.** Summary of Crystal, Intensity Collection, and Refinement Data for  $K_2[Co_2(C_6H_5O_7)_2(H_2O)_4] \cdot 6H_2O$  (**1**) and  $Na_2[Co_2(C_6H_5O_7)_2(H_2O)_4] \cdot 6H_2O$  (**2**)

parameters	<b>1</b>	<b>2</b>
empirical formula	$C_{12}H_{30}K_2O_{24}Co_2$	$C_{12}H_{30}Na_2O_{24}Co_2$
fw	754.42	722.20
temp, K	298	298
wavelength ( $\lambda$ , $\text{\AA}$ )	Mo K $\alpha$ (0.710 73)	Mo K $\alpha$ (0.710 73)
space group	$P2_1/n$	$P2_1/c$
$a$ , $\text{\AA}$	10.348(5)	9.234(4)
$b$ , $\text{\AA}$	11.578(6)	11.913(4)
$c$ , $\text{\AA}$	12.138(6)	11.728(6)
$\alpha$ , deg		
$\beta$ , deg	112.62(2)	99.93(2)
$\gamma$ , deg		
$V$ , $\text{\AA}^3$	1342(1)	1271(1)
$Z$	2	2
$D_{calc}/D_{meas}$ ( $\text{Mg m}^{-3}$ )	1.866/1.85	1.887/1.87
abs. coeff ( $\mu$ ), $\text{mm}^{-1}$	1.647	1.446
$F(000)$	772	740
range of $h, k, l$	$-11 \rightarrow 12, 0 \rightarrow 13,$ $-14 \rightarrow 0$	$-10 \rightarrow 10, 0 \rightarrow 14,$ $0 \rightarrow 13$
data/restraints/params	2357/0/241	2224/0/241
goodness-of-fit on $F^2$	1.071	1.057
R indices	$R = 0.0333,$ $R_w = 0.0859^a$	$R = 0.0297,$ $R_w = 0.0792^b$
R indices (all data) <sup>c</sup>	$R = 0.0385,$ $R_w = 0.0898$	$R = 0.0343,$ $R_w = 0.0833$

<sup>a</sup> 2105 reflections  $I > 2\sigma(I)$ . <sup>b</sup> 1968 reflections  $I > 2\sigma(I)$ . <sup>c</sup>  $R = (\sum ||F_o| - |F_c||) / (\sum |F_o|)$ ,  $R_w = (\sum [w(F_o^2 - F_c^2)^2]) / (\sum [w(F_o^2)^2])^{1/2}$ .

ligand, and concurrently provided the necessary counterions for the balance of charge generated on the subsequently isolated complexes **1** and **2**.



In the described isolation procedures of the syntheses reactions, both water/ethanol mixtures as well as slow evaporation were effective in inducing precipitation of the desired colored products. In all cases, the yields of the reactions were  $\sim$ 50% or greater.

In all of the employed methods for the syntheses of **1** and **2**, the isolated products were crystalline and were used as such for further spectroscopic and crystallographic studies. Elemental analyses on the derived products suggested the formulation  $K_2[Co_2(C_6H_5O_7)_2(H_2O)_4] \cdot 6H_2O$  for **1** and  $Na_2[Co_2(C_6H_5O_7)_2(H_2O)_4] \cdot 6H_2O$  for **2**. Further X-ray crystallographic investigations confirmed the above analytical formulations. The crystals of **1** and **2** isolated from reaction 1 were stable in the air for long periods of time. Both complexes **1** and **2** were soluble in aqueous solutions at pH  $\sim$ 5.

**Crystal Structure.** The X-ray three-dimensional structure determination of complexes **1** and **2** was carried out.

(20) Irving, H.; Miles, M. G.; Pettit, L. D. *Anal. Chim. Acta* **1967**, *38*, 475–488.

(21) Zekany, L.; Nagypal, I.; Peintler, G. *PSEQUAD for Chemical Equilibria*; Technical Software Distributions: Baltimore, MD, 1991.

(22) Sheldrick, G. M. In *SHELXS-86: Structure Solving Program*; University of Göttingen: Göttingen, Germany, 1986.

(23) Sheldrick, G. M. In *SHELXL-97: Crystal Structure Refinement*; University of Göttingen: Göttingen, Germany, 1997.

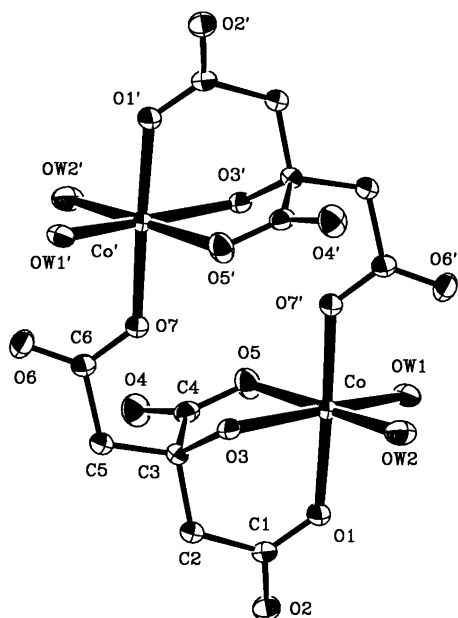


**Figure 1.** Structure of the  $[\text{Co}_2(\text{C}_6\text{H}_5\text{O}_7)_2(\text{H}_2\text{O})_4]^{2-}$  anion with the atom labeling scheme in **1**. Thermal ellipsoids are drawn by ORTEP and represent 50% probability surfaces.

Complex **1** crystallizes in the monoclinic space group  $P2_1/n$  with 2 molecules in the unit cell, whereas complex **2** crystallizes in the monoclinic space group  $P2_1/c$  with two molecules in the unit cell. The ORTEP diagram of the anion  $[\text{Co}_2(\text{C}_6\text{H}_5\text{O}_7)_2(\text{H}_2\text{O})_4]^{2-}$  is shown in Figure 1. A selected list of interatomic bond distances and angles for **1** and **2** is given in Table 2. Both structures consist of discrete centrosymmetric  $[\text{Co}_2(\text{C}_6\text{H}_5\text{O}_7)_2(\text{H}_2\text{O})_4]^{2-}$  anions and cations. The anion is a dinuclear complex, comprised of two Co(II) ions linked together with two citrate ligands. Each citrate ligand is triply deprotonated, and as such, it coordinates to the Co(II) ion, thus giving rise to two distorted octahedral units within the dimer. Furthermore, due to the presence of high-spin  $d^7$  electronic configuration in the Co(II) ions of **1** and **2**, the Jahn–Teller effect emerges dominant, resulting in a tetragonal distortion of both octahedral units. In each generated octahedron, the citrate ligand binds in a tridentate fashion. It employs one of the terminal carboxylate groups as well as the central carboxylate and alcoholic OH groups, to effectively coordinate to the metal ion. The remaining terminal carboxylate group does not participate in the coordination to the same metal ion. Instead, it spans over to the second octahedral complex of the dimer and coordinates to the second Co(II) metal ion. Another feature worth noting in the structures of **1** and **2** is the protonation state of the alcoholic oxygen on the citrate ligand bound to the Co(II) ion. Both in the case of the reported complexes **1** and **2** as well as in the case of the mononuclear complex  $[\text{Co}(\text{C}_6\text{H}_5\text{O}_7)_2]^{4-}$ ,<sup>16</sup> the central alcoholic oxygen retains its proton upon coordination to the metal ion. Two water molecules are also present in each octahedron generated via coordination of the citrate ligand to Co(II).

Comparisons of the bond distances and angles in **1** and **2** with corresponding structural parameters in other octahedral Co(II)- and Ni(II)-containing complexes are given in Table

**Table 2.** Bond Lengths (Å) and Angles (deg) for the Complexes  $\text{K}_2[\text{Co}_2(\text{C}_6\text{H}_5\text{O}_7)_2(\text{H}_2\text{O})_4] \cdot 6\text{H}_2\text{O}$  (**1**) and  $\text{Na}_2[\text{Co}_2(\text{C}_6\text{H}_5\text{O}_7)_2(\text{H}_2\text{O})_4] \cdot 6\text{H}_2\text{O}$  (**2**)<sup>a</sup>

	<b>1</b>	<b>2</b>
Co–O(1)	2.042(2)	2.069(2)
Co–O(3)	2.194(2)	2.169(2)
Co–O(5)	2.065(2)	2.044(2)
Co–O(7')	2.045(2)	2.044(2)
Co–OW1	2.117(2)	2.134(2)
Co–OW2	2.095(2)	2.128(2)
O(1)–C(1)	1.264(3)	1.271(3)
C(1)–O(2)	1.242(3)	1.238(3)
O(3)–C(3)	1.457(3)	1.459(3)
C(4)–O(4)	1.234(3)	1.223(3)
O(5)–C(4)	1.269(3)	1.270(3)
C(6)–O(6)	1.231(3)	1.231(3)
O(7)–C(6)	1.281(3)	1.283(3)
C(1)–C(2)	1.529(3)	1.518(3)
C(2)–C(3)	1.524(3)	1.527(3)
C(3)–C(4)	1.546(3)	1.540(3)
C(3)–C(5)	1.532(3)	1.524(3)
C(5)–C(6)	1.524(3)	1.518(3)
O(5)–Co–O(3)	77.17(7)	78.25(7)
O(5)–Co–OW1	92.03(8)	92.60(7)
OW2–Co–OW1	92.85(9)	88.72(7)
OW2–Co–O(3)	98.18(8)	100.37(7)
O(1)–Co–O(3)	84.71(7)	85.52(7)
O(5)–Co–O(1)	90.98(8)	89.70(8)
O(1)–Co–OW1	90.12(8)	92.32(7)
O(1)–Co–OW2	91.33(9)	88.77(8)
O(7')–Co–O(3)	94.08(7)	88.70(7)
O(5)–Co–O(7')	87.26(8)	89.41(7)
O(7')–Co–OW1	90.78(7)	93.43(7)
O(7')–Co–OW2	90.34(9)	92.00(7)
O(7')–Co–O(1)	178.06(7)	174.22(7)
O(2)–C(1)–O(1)	123.1(2)	123.8(2)
O(2)–C(1)–C(2)	116.0(2)	116.2(2)
O(1)–C(1)–C(2)	120.9(2)	120.0(2)
C(1)–C(2)–C(3)	118.0(2)	118.2(2)
O(3)–C(3)–C(5)	109.4(2)	109.4(2)
O(3)–C(3)–C(2)	108.4(2)	108.0(2)
C(5)–C(3)–C(2)	111.0(2)	109.8(2)
O(3)–C(3)–C(4)	109.5(2)	109.9(2)
C(5)–C(3)–C(4)	109.8(2)	111.1(2)
C(2)–C(3)–C(4)	108.8(2)	108.7(2)
O(4)–C(4)–O(5)	125.3(2)	125.2(2)
O(4)–C(4)–C(3)	118.0(2)	117.8(2)
O(5)–C(4)–C(3)	116.6(2)	116.9(2)
C(6)–C(5)–C(3)	112.1(2)	114.2(2)
O(6)–C(6)–O(7)	124.3(2)	125.0(2)
O(6)–C(6)–C(5)	121.2(2)	119.2(2)
O(7)–C(6)–C(5)	114.5(2)	115.8(2)

<sup>a</sup> Symmetry transformations used to generate equivalent atoms (with primes): (**1**)  $-x, -y, -z$ ; (**2**)  $-x + 1, -y + 1, -z$ .

3.<sup>24–28</sup> The Co–O distances and angles observed in **1** and **2** are comparable with those seen in other dinuclear and mononuclear metal ion citrate complexes. Of all the angles formed in the two octahedra, worth noting is the O(3)–Co–O(5) angle, which is 77.17(7) and 78.25(7)° in **1** and **2**, respectively. This small angle is similar to the corresponding angle in  $\text{K}_2[\text{Ni}_2(\text{C}_6\text{H}_5\text{O}_7)_2(\text{H}_2\text{O})_4] \cdot 4\text{H}_2\text{O}$ ,<sup>24</sup> and it denotes the distort-

(24) Baker, E. N.; Baker, H. M.; Anderson, B. F.; Reeves, R. D. *Inorg. Chim. Acta* **1983**, *78*, 281–285.

(25) Zhou, Z.-H.; Lin, Y.-J.; Zhang, H.-B.; Lin, G.-D.; Tsai, K.-R. *J. Coord. Chem.* **1997**, *42*, 131–141.

(26) Chen, X.-M.; Mak, T. C. W. *Acta Crystallogr.* **1992**, *C48*, 1211–1214.

(27) Bkouche-Waksman, I.; L'Haridon, P. *Bull. Soc. Chim. Fr.* **1979**, *1–2*, 150–153.

(28) Kryger, L.; Rasmussen, S. E. *Acta Chem. Scand.* **1972**, *26*, 2349–2359.

**Table 3.** Bond Distances and Angles in Co(II) and Ni(II) Compounds

Compound	distances (Å)		angles (deg)	
	Co–O	M···M	(O–Co–O) <sub>equatorial</sub> <sup>e</sup>	(O–Co–O) <sub>apical</sub> <sup>f</sup>
K <sub>2</sub> [Co <sub>2</sub> (C <sub>6</sub> H <sub>5</sub> O <sub>7</sub> ) <sub>2</sub> (H <sub>2</sub> O) <sub>4</sub> ]·6H <sub>2</sub> O ( <b>1</b> ) <sup>a,b</sup>	2.042(2)–2.194(2)	5.247(1)	87.26(8)–91.33(9)	77.17(7)–98.18(8)
Na <sub>2</sub> [Co <sub>2</sub> (C <sub>6</sub> H <sub>5</sub> O <sub>7</sub> ) <sub>2</sub> (H <sub>2</sub> O) <sub>4</sub> ]·6H <sub>2</sub> O ( <b>2</b> ) <sup>a,b</sup>	2.044(2)–2.169(2)	5.361(1)	88.77(7)–92.00(7)	78.25(7)–100.37(7)
K <sub>2</sub> [Ni <sub>2</sub> (C <sub>6</sub> H <sub>5</sub> O <sub>7</sub> ) <sub>2</sub> (H <sub>2</sub> O) <sub>4</sub> ]·4H <sub>2</sub> O <sup>24,b</sup>	2.036(3)–2.125(3)	5.364(1)	78.5(1)–94.5(1)	86.8(1)–95.2(1)
(NH <sub>4</sub> ) <sub>2</sub> [Ni <sub>2</sub> (C <sub>6</sub> H <sub>5</sub> O <sub>7</sub> ) <sub>2</sub> (H <sub>2</sub> O) <sub>4</sub> ]·2H <sub>2</sub> O <sup>25,b</sup>	2.020(3)–2.074(2)	NA <sup>g</sup>	81.53(9)–96.7(2)	86.12(9)–92.69(9)
(NH <sub>4</sub> ) <sub>4</sub> [Co(C <sub>6</sub> H <sub>5</sub> O <sub>7</sub> ) <sub>2</sub> ] <sup>16,b</sup>	2.051(2)–2.157(2)		88.63(8)–91.37(8)	74.80(7)–105.20(7)
[Co <sup>II</sup> {(CH <sub>3</sub> ) <sub>3</sub> NCH <sub>2</sub> COO} <sub>2</sub> (H <sub>2</sub> O) <sub>4</sub> ]Cl <sub>2</sub> ·4H <sub>2</sub> O <sup>26,c</sup>	2.087(2)–2.101(2)		89.2(1)–90.8(1)	87.5(1)–92.5(1)
[Co <sup>II</sup> {C <sub>2</sub> H <sub>5</sub> OH} <sub>6</sub> ][CoBr <sub>4</sub> ] <sup>27</sup>	2.01(3)–2.14(3)		88(1)–93(1)	86(1)–92(1)
[Co <sup>II</sup> (COOCH <sub>2</sub> CHOHCOO)]·3H <sub>2</sub> O <sup>28,d</sup>	2.067(3)–2.136(3)		87.34(12)–94.71(13)	76.82(12)–101.02(13)

<sup>a</sup> This work. <sup>b</sup> C<sub>6</sub>H<sub>5</sub>O<sub>7</sub><sup>2-</sup> = citrate. <sup>c</sup> (CH<sub>3</sub>)<sub>3</sub>N<sup>+</sup>CH<sub>2</sub>COO<sup>-</sup> = trimethylammonium acetate. <sup>d</sup> (COOCH<sub>2</sub>CHOHCOO)<sup>2-</sup> = malate. <sup>e</sup> O–Co–O angle range in the equatorial plane. <sup>f</sup> O–Co–O angles between the axial and equatorial ligands. <sup>g</sup> NA = not available.

tion brought about by the small bite of the five-membered ring provided by the central alcoholic and carboxylate groups, when the latter bind to the metal ion. The Co···Co distance in the dimers of **1** and **2** is 5.247(1) and 5.361(1) Å, respectively, very similar to that observed in K<sub>2</sub>[Ni<sub>2</sub>(C<sub>6</sub>H<sub>5</sub>O<sub>7</sub>)<sub>2</sub>(H<sub>2</sub>O)<sub>4</sub>]·4H<sub>2</sub>O (5.364(1) Å).<sup>24</sup> In general, the [Ni<sub>2</sub>(C<sub>6</sub>H<sub>5</sub>O<sub>7</sub>)<sub>2</sub>(H<sub>2</sub>O)<sub>4</sub>]<sup>2-</sup> dimer,<sup>24,25</sup> reported in two different crystal structures, possesses structural features very similar to those seen in [Co<sub>2</sub>(C<sub>6</sub>H<sub>5</sub>O<sub>7</sub>)<sub>2</sub>(H<sub>2</sub>O)<sub>4</sub>]<sup>2-</sup>. Detailed examination of the individual octahedral unit [Co(C<sub>6</sub>H<sub>5</sub>O<sub>7</sub>-A)-(H<sub>2</sub>O)<sub>2</sub>(O-cit-B)]<sup>2-</sup> (where A and B represent the two citrate ligands) in the dimer shows that the bond distances and angles are also similar to those observed in the corresponding monomeric octahedral complex anion [Co(C<sub>6</sub>H<sub>5</sub>O<sub>7</sub>)<sub>2</sub>]<sup>4-</sup>. Furthermore, by comparison of the structural units in the dimers **1** and **2** with that in the mononuclear complex [Co(C<sub>6</sub>H<sub>5</sub>O<sub>7</sub>)<sub>2</sub>]<sup>4-</sup>, it becomes evident that a 1:1 Co(II):citrate stoichiometry exists in the dimer in contrast to the dominant 1:2 Co(II):citrate stoichiometry observed in [Co(C<sub>6</sub>H<sub>5</sub>O<sub>7</sub>)<sub>2</sub>]<sup>4-</sup>. Conceivably, upon adoption of the 1:1 stoichiometry, the monomeric unit in both **1** and **2** generates empty coordination sites in the octahedral assembly, which are filled by the pendant terminal carboxylate of an adjacent Co(II)–citrate monomer and two water molecules from the solvent medium. Hence, the dinuclear structure emerges in the solid state.

The potassium and sodium cations counterbalance efficiently the anionic charge of [Co<sub>2</sub>(C<sub>6</sub>H<sub>5</sub>O<sub>7</sub>)<sub>2</sub>(H<sub>2</sub>O)<sub>4</sub>]<sup>2-</sup> in complexes **1** and **2**, respectively. The potassium ions in **1** are in contact with the carboxylate oxygens of the citrate anion as well as bound and lattice water oxygens at distances in the range 2.634(2)–3.231(2) Å (seven contacts). The sodium ions in **2** are in contact with water molecules of crystallization and coordinated water molecules as well as with oxygens from the citrates in a distance range 2.196(2)–2.590(2) Å (six contacts). Furthermore, these two cations in the respective lattices of **1** and **2** help link the anionic assemblies together as well as with the water molecules of crystallization. Consequently, a three-dimensional network of hydrogen bonds forms that involves citrate carboxylate oxygens as well as lattice water molecules and water molecules bound to the Co(II) ions. It is very likely that the formation of such an extensive hydrogen-bonding network leads to stable lattices in complex **1** and **2**.

**Electronic Spectroscopy.** Upon dissolution of **1** in water the UV/visible spectrum shows a major peak at  $\lambda_{\max} = 516$

nm ( $\epsilon = 10.4$ ), subtly distinguishable shoulders around 460 ( $\epsilon \sim 6$ ) and 480 ( $\epsilon \sim 9$ ), and another shoulder around 615 nm ( $\epsilon = 1$ ). The absorption features are most likely d–d transitions in origin, typical for a high-spin Co(II) d<sup>7</sup> octahedral species.<sup>29</sup> The band at 516 nm could be tentatively assigned to the <sup>4</sup>T<sub>1g</sub> → <sup>4</sup>T<sub>1g</sub>(P) transition, with the weak absorption appearing as a shoulder around 615 nm also tentatively attributed to the <sup>4</sup>T<sub>1g</sub> → <sup>4</sup>A<sub>2g</sub> transition.<sup>30</sup> The observed multiple structure in the spectrum confirms literature reports ascribing its origin to (a) admixture of spin forbidden transitions to doublet states derived from <sup>2</sup>G and <sup>2</sup>H, (b) spin–orbit coupling, and (c) vibrational or low-symmetry components. No further definitive assignments can, therefore, be made due to the absence of detailed studies and analyses. To check the solution state of complex **1** following dissolution, the UV/visible spectrum of the complex was recorded at different concentrations in the range 1–100 mM at pH ~6. The Lambert–Beer law at  $\lambda_{\max} = 516$  nm was found to be valid, indicating the presence of a single species and excluding the possibility of a monomer–dimer equilibrium in this concentration range. Similar measurements were carried out at pH ~10, at a 2-fold ligand excess (to avoid precipitation), where the speciation calculations (vide infra) indicated the formation of either the monomeric species [CoLH<sub>-1</sub>]<sup>2-</sup> or its dimeric form. The Lambert–Beer law at the observed  $\lambda_{\max} = 534$  nm was again valid suggesting the formation of a single species in this case as well.

**Infrared Spectroscopy.** The FT-infrared spectra of **1** and **2** were recorded in KBr. They reveal the presence of resonances attributed to vibrationally active carbonyls of the citrate carboxylate ligands. In both **1** and **2**, the antisymmetric stretching vibrations  $\nu_{\text{as}}(\text{COO}^-)$  appear between 1677 and 1581 cm<sup>-1</sup> for **1** and 1677 and 1582 cm<sup>-1</sup> for **2**. The symmetric stretching vibrations  $\nu_{\text{s}}(\text{COO}^-)$  appear between 1418 and 1390 cm<sup>-1</sup> for **1** and 1418 and 1387 cm<sup>-1</sup> for **2**. In both **1** and **2** the frequencies of the bands of the antisymmetric and symmetric stretching vibrations are shifted to lower values compared to the corresponding vibrations in free citric acid, thus indicating a change in the coordination status of the carboxylates in the citrate ligand. The frequency difference,  $\Delta(\nu_{\text{as}}(\text{COO}^-) - \nu_{\text{s}}(\text{COO}^-))$ ,<sup>31,32</sup> in both **1** and **2**

(29) Drago, R. S. In *Physical Methods in Chemistry*; W. B. Saunders W. B. Co.: Philadelphia, PA, 1977; pp 359–410.

(30) Lever, A. B. P. In *Inorganic Electronic Spectroscopy*, 2nd ed.; Elsevier: Amsterdam, 1984; pp 480–490.

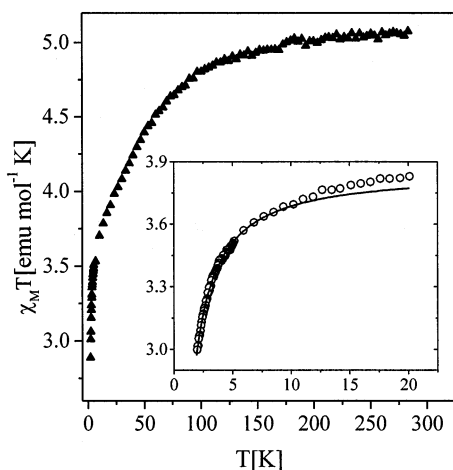


**Figure 2.** Temperature dependence of the magnetic susceptibility in the form of  $\chi_M T$  vs  $T$  in the temperature range 2–290 K at 0.2 T. The inset picture represents the best fit in the temperature range 2–20 K, according to eq 1.

is greater than  $200\text{ cm}^{-1}$ , indicating the presence of deprotonated carboxylate groups coordinated to the metal in a monodentate fashion. This assertion is further proven by the X-ray crystal structure determination of **1** and **2**. All of the aforementioned assignments are in consonance with the FT-IR features of the mononuclear species  $(\text{NH}_4)_4[\text{Co}(\text{C}_6\text{H}_5\text{O}_7)_2]^{16}$  as well as other metal ion citrate complexes investigated so far.<sup>33–36</sup>

**Magnetic Susceptibility Measurements.** Magnetic susceptibility measurements on complex **1** were carried out at different magnetic fields and in the temperature range 1.90–290 K. Figure 2 shows the  $\chi_M T$  versus  $T$  magnetic susceptibility data at 0.2 T.

The  $\chi_M T$  values decrease from  $5.12\text{ emu}\cdot\text{mol}^{-1}\cdot\text{K}$  at 290 K to  $2.97\text{ emu}\cdot\text{mol}^{-1}\cdot\text{K}$  at 1.9 K. The high-temperature value of  $\chi_M T$  is higher than  $3.75\text{ emu}\cdot\text{mol}^{-1}\cdot\text{K}$ , the value that would be expected for a Co(II) dinuclear system with an  $S_1 = S_2 = 3/2$ . This behavior is consistent with the presence of a significant orbital contribution to the anisotropic nature of the Co(II) system investigated. Co(II) can be described by the low-lying spin-doublet  $S = 1/2$ , which is anisotropic in Co(II). It must be pointed out that in Co(II) this effective spin doublet arises from the splitting of the  $^4T_1$  term through spin–orbit coupling and local distortion of the octahedral sites. To verify the magnitude of the exchange interaction in **1**, if any, the general quantum mechanical operator can be written explicitly as

$$H = -(J_z S_1^z S_2^z + J_x S_1^x S_2^x + J_y S_1^y S_2^y) + B \cdot g_i \cdot S_i \quad (\text{eq. 1})$$

where  $i = 1, 2$ , the effective spin is  $S_1 = S_2 = 1/2$ , and axial

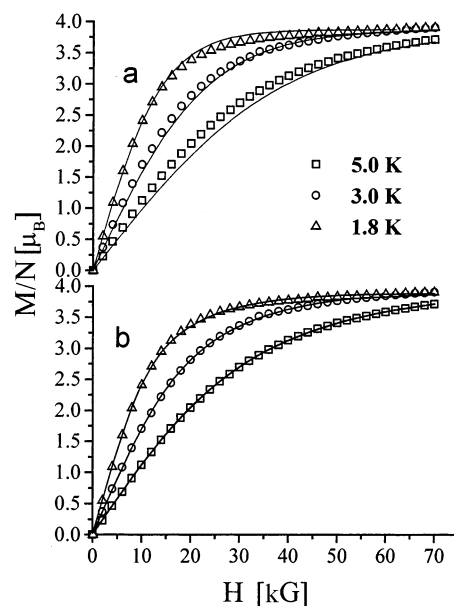


**Figure 3.** Magnetization measurements in the field range 0–7 T and at various temperatures: (a) solid lines represent the theoretical magnetization curves for two independent spins, each with  $S = 1/2$  and  $g = 3.87$ ; (b) solid lines represent simulation curves (see text for details).

$J$  ( $J_x = J_y, J_z$ ) and  $g$  ( $g_x = g_y, g_z$ ) values are considered. Furthermore, the lack of many signals in the EPR spectra indicates that there is only one  $g$  tensor, the same for both Co(II) ions. This anisotropic model limits its applicability in the low-temperature range ( $T < 30\text{ K}$ ).<sup>37,38</sup> There, only the lowest lying spin doublet of Co(II) is significantly populated, yet that is adequate to obtain useful information on the exchange parameter  $J$ . When  $J_z \neq 0$  and  $J_x = J_y = 0$ , the system is in the Ising limit. When  $J_z = 0$  and  $J_x = J_y \neq 0$ , the system is in the XY limit. The best fit of the experimental data to the expression for the magnetic susceptibility derived from this model gives an exchange parameter  $J_z = -0.94(5)\text{ cm}^{-1}$ ,  $g_z = 6.2(2)$ ,  $J_{xy}/J_z = 0.13$ , and  $g_{xy}/g_z = 0.46$  and is shown as a solid line in the inset of Figure 2. If we have in mind that  $J = (J_x + J_y + J_z)/3$ , the value of  $J$  for this model is  $J = -0.4\text{ cm}^{-1}$ , which is in accordance with a small anisotropic antiferromagnetic interaction. To test the validity of the fitting values, the magnitude of the anisotropy for the Co···Co interaction was investigated. Generally, that is given by  $J_{xy}/J_z \sim (g_{xy}/g_z)^2$ , where  $J_{xy}$  and  $J_z$  are the parallel and perpendicular exchange components to the spin direction ( $J$  has been assumed to be axial).<sup>38,39</sup> On the basis of the values obtained from the fitting process, an agreement arises between the two terms of the aforementioned mathematical relationship. To further investigate the fitting process, simulations of the magnetization data (vide infra) were carried out, using the values obtained from the fitting. The results are shown in Figure 3b. Here too, the observed fits are in agreement with the experimental curves.

- (31) Djordjevic, C.; Lee, M.; Sinn, E. *Inorg. Chem.* **1989**, *28*, 719–723.  
 (32) Deacon, G.; Philips, R. *J. Coord. Chem. Rev.* **1980**, *33*, 227–250.  
 (33) Matzapetakis, M.; Kourgiantakis, M.; Dakanali, M.; Raptopoulou, C. P.; Terzis, A.; Lakatos, A.; Kiss, T.; Iordanidis, L.; Mavromoustakos, T.; Salifoglou, A. *Inorg. Chem.* **2001**, *40*, 1734–1744.  
 (34) Kourgiantakis, M.; Matzapetakis, M.; Raptopoulou, C. P.; Terzis, A.; Salifoglou, A. *Inorg. Chim. Acta* **2000**, *297*, 134–138.  
 (35) Matzapetakis, M.; Karligiano, N.; Bino, A.; Dakanali, M.; Raptopoulou, C. P.; Tangoulis, V.; Terzis, A.; Giapintzakis, J.; Salifoglou, A. *Inorg. Chem.* **2000**, *39*, 4044–4051.

- (36) Matzapetakis, M.; Raptopoulou, C. P.; Terzis, A.; Lakatos, A.; Kiss, T.; Salifoglou, A. *Inorg. Chem.* **1999**, *38*, 618–619.  
 (37) Pastor, N. C.; Serra, J. B.; Coronado, E.; Pourroy, G.; Baker, L. C. *W. J. Am. Chem. Soc.* **1992**, *114*, 10380–10383.  
 (38) Garcia, C. J. G.; Coronado, E.; Almenar, J. B. *Inorg. Chem.* **1992**, *31*, 1667–1673.

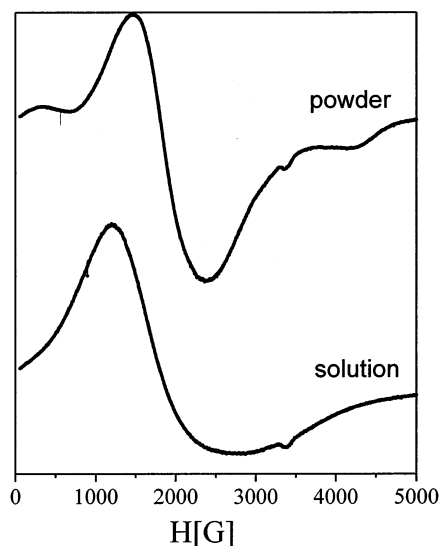


**Figure 4.** X-Band EPR spectra of complex **1** in a powder sample and in solution, at 4 K.

Magnetization measurements on **1** were run at three different temperatures and in the field range 0–7 T. The derived data are shown in the form of  $M/N$  [ $\mu_B$ ] vs  $H$  [kG] in Figure 3a. The large value of the  $M_{\text{saturation}}$  ( $4 \mu_B$  at 1.8 K) is in accordance with a very small interaction between the two Co(II) magnetic centers. To verify the above contention, simulations were carried out assuming two independent spins in the dinuclear complex, each with  $S = 1/2$ . The solid lines represent the theoretical magnetization curves for a system with two independent spins each with  $S = 1/2$  and an effective  $g$  value equal to 3.87. They clearly reveal the small antiferromagnetic exchange interaction between the cobalt(II) ions (Figure 3a).

**Electron Paramagnetic Resonance.** To explore the existence of a weak interaction between the Co(II) centers in complex **1**, X-band powder and solution EPR experiments were carried out in the temperature range 4–40 K (Figure 4). As a consequence of the fast spin–lattice relaxation time of high-spin Co(II), signals were observed only below 40 K. The  $g$  values obtained from the powder EPR spectrum of **1** are  $g_z = 13.7$ ,  $g_x = 3.63$ , and  $g_y = 1.6$ . An important piece of information pertaining to the nature of the exchange interaction emerges from the  $g$  values of the single cobalt(II) ion: if  $g_z > g_x, g_y$ , the ion is closer to the Ising limit. If  $g_x, g_y > g_z$ , the system is closer to the XY limit. The conditions for observing  $g_z > g_x, g_y$  were given earlier by Abragam and Bleaney, using a crystal field approach.<sup>39</sup> It was, then, found that in the Ising limit  $g_z = 8–9$  and  $g_x = g_y = 0$ , while for the XY limit  $g_{xy} = 4$  and  $g_z = 2$ . The values observed here for complex **1** are beyond every limit, thus indicating that an interaction between the two Co(II) octahedral centers does arise. It is interesting to note that, in solution, the dimer seems to break into monomers, in view of the fact that the derived signal exhibits an isotropic  $g$  value equal to 3.75. This value is very close to the one derived from the magnetization measurements, where an effective-spin  $S = 1/2$  was used to simulate the magnetic

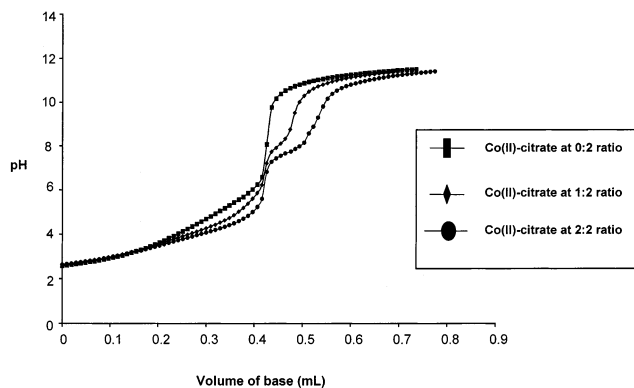


**Figure 5.** Experimental titration points and calculated titration curves (solid lines) in the Co(II)–citric acid system at  $c_{\text{ligand}} = 0.002$  M and at 0:2, 1:2, and 2:2 metal ion to ligand molar ratios.

behavior. Such a  $g$  value is commonly observed in the case of octahedral Co(II) centers.

**Speciation Studies.** Potentiometric titrations of the ligand citric acid alone and Co(II) with citric acid in various metal ion to ligand molar ratios were carried out. Some of the obtained titration curves are shown in Figure 5. The titration curves were evaluated by different potential speciation models. The best fit between the experimental and calculated titration curves was obtained by considering the species  $[\text{CoLH}]^0$  ( $\text{LH} = \text{C}_6\text{H}_6\text{O}_7^{2-}$ ),  $[\text{CoL}]^-$  ( $\text{L} = \text{C}_6\text{H}_5\text{O}_7^{3-}$ ),  $[\text{CoL}_2]^{4-}$ , and  $[\text{CoLH}_{-1}]^{2-}$  ( $\text{LH}_{-1} = \text{C}_6\text{H}_4\text{O}_7^{4-}$ ) or its dimeric form  $[(\text{CoLH}_{-1})_2]^{4-}$ . The titration data could be equally well evaluated by two speciation models, differing in the nuclearity of the deprotonated species  $[\text{CoLH}_{-1}]^{2-}$ . Other complexes, like 1:3 Co(II):citrate complexes or other protonated or deprotonated species were rejected by the computer program during the calculation process. As the complex isolated in the solid state is a dinuclear species, the nuclearity of the complex in solution was carefully checked. When the presence of the dinuclear species  $[\text{Co}_2\text{L}_2]^{2-}$  was evoked in addition to the mononuclear species  $[\text{CoL}]^-$ , the former species was rejected. When only the dinuclear species was assumed with the monomer omitted from the speciation model, the fit between the experimental and the calculated titration curves decreased considerably (by  $\sim 60\%$ ). These facts, along with the electronic spectra, which indicate the formation of a single species at  $\text{pH} \sim 6$  (vide supra), suggest that, in all likelihood, formation of the dinuclear species  $[\text{Co}_2\text{L}_2]^{2-}$  in solution, at least in the 1–100 mM concentration range, can be excluded. The stability constants of the complexes formed are listed in Table 4. The pH range of their optimal formation is also reported. Earlier speciation models<sup>40</sup> included only 1:1 complexes in various protonation states (no bis complexes have been detected so far). Despite the aforementioned difference, the speciation model suggested here, in conjunction with the stability constants, is in reasonably good agreement with those reported in the literature.<sup>40</sup>

(39) Abragam, A.; Bleaney, B. In *Electron Paramagnetic Resonance of Transition Ions*; Clarendon Press: Oxford, U.K., 1970.

(40) Pettit, L. D.; Powell, H. K. J. In *Stability Constant Database*, 2nd release; IUPAC and Academic Software: London, Otley, 1997.

**Table 4.** Proton ( $\log K$ ) and Cobalt(II) Complex Formation Constants ( $\log \beta$ ) of Citric Acid at  $I = 0.20$  M (KCl) and  $25^\circ\text{C}^a$ 

	citric acid	model 1	model 2	pH range for each species
$\log K(\text{HL})$	5.59(1)			
$\log K(\text{H}_2\text{L})$	4.26(1)			
$\log K(\text{H}_3\text{L})$	2.87(2)			
$\log \beta(\text{CoLH})$		8.28(1)	8.27(1)	3–5
$\log \beta(\text{CoL})$		4.63(1)	4.64(1)	4–8
$\log \beta(\text{CoLH}_{-1})$			-3.23(2)	>7
$\log \beta(\text{CoL}_2)$		7.01(3)	6.90(5)	5–8
$\log \beta(\text{Co}_2\text{L}_2\text{H}_{-2})$		-3.52(2)		>7
fitting <sup>b</sup>		0.00271	0.00336	
no. of pts		600	600	

<sup>a</sup> Charges from the various species are omitted for clarity. <sup>b</sup> Goodness of fit between the experimental and the calculated titration curves expressed in mL of titrant.

The pH-titrimetric data were evaluated on the premise that complex formation between citrate and Co(II) ion proceeds through the carboxylate moieties and the central alcoholic group. Close inspection of Figure 5 reveals immediately and clearly the third dissociating carboxylate proton on the tricarboxylic acid, with the previous two carboxylate protons dissociating at lower pH values. Deviations between the titration curves obtained in the presence and absence of Co(II), in the acidic pH range, clearly indicate formation of the 1:1 mononuclear species  $[\text{CoLH}]^0$  ( $\text{LH} = \text{C}_6\text{H}_6\text{O}_7^{2-}$ ). As pH increases, two more species,  $[\text{CoL}]^-$  and  $[\text{CoL}_2]^{4-}$ , grow into the potential biodistribution scheme, with the former species being the predominant mononuclear entity in solution. The  $[\text{CoL}]^-$  species contains one triply deprotonated citrate ligand bound to the metal ion, while  $[\text{CoL}_2]^{4-}$  contains two triply deprotonated citrate ligands attached to the cobalt ion. A 1:2 metal ion to ligand stoichiometry strongly proposes an octahedral geometry for  $[\text{CoL}_2]^{4-}$ . The binding mode of citrate in these complexes can be either through the three carboxylates or through one of the terminal carboxylates, the central carboxylate, and the protonated alcoholic OH, while the other terminal carboxylate does not participate in the coordination around Co(II). This latter binding mode occurs in the solid state in complex  $[\text{Co}(\text{C}_6\text{H}_5\text{O}_7)_2]^{4-}$ .<sup>16</sup> Interestingly, the tridentate carboxylate coordination of citrate is not favored for other metal ions either, as that is attested to in the case of metals such as Cu(II),<sup>41</sup> Al(III),<sup>42</sup> or VO(II).<sup>43</sup> As the ratio of the stepwise stability constants  $\log(K(\text{CoL})/K(\text{CoL}_2)) \sim 2.3$  indicates, coordination of the second citrate molecule to Co(II) is rather hindered, very likely due to the significant electrostatic repulsion between the reacting species  $[\text{CoL}]^-$  and  $\text{L}^{3-}$ .

Further increase in the pH of the solution yields equivocal results pertaining to species such as  $[\text{CoLH}_{-1}]^{2-}$  (see model 2 in Table 4). In this complex, the citrate ligand may be bound to the metal ion as a quadruply deprotonated moiety, through the Co(II) induced deprotonation and subsequent coordination of the central alcoholic function. Alternatively,

the same stoichiometry may be obtained through deprotonation of a coordinated water molecule in the coordination sphere of the metal ion. The first hydrolysis constant of  $[\text{Co}(\text{H}_2\text{O})_6]^{2+}$  is  $\text{p}K \sim 9.8$ , about 2 orders of magnitude greater than the  $\text{p}K(\text{CoL}) = 7.86$ . Since such a significant increase in the acidity of a coordinated water in complex  $[\text{CoL}]^-$  cannot be expected (on the contrary some decrease in the acidity is reasonable), the Co(II)-induced deprotonation of the central alcoholic OH, resulting in a  $(\text{CO}_2^-)_{\text{terminal}}, (\text{CO}_2^-)_{\text{central}}, \text{O}^-_{\text{central}}$  binding mode, with the other terminal carboxylate being noncoordinated, may be more probable. To this end, corroborating evidence comes from the electronic spectra of the employed solutions. The spectra, in this case, display some pH dependence: in an equimolar Co(II)–citrate solution at  $\text{pH} \sim 6$ , where complex  $[\text{CoL}]^-$  predominates,  $\lambda_{\text{max}}$  is observed at 516 nm ( $\epsilon = 10.4 \text{ M}^{-1} \text{ cm}^{-1}$ ), while, at  $\text{pH} \sim 10$ , where complex  $[\text{CoLH}_{-1}]^{2-}$  is the only species present,  $\lambda_{\text{max}}$  shifts to 534 nm ( $\epsilon = 15.3 \text{ M}^{-1} \text{ cm}^{-1}$ ) and a new band occurs at  $\lambda_{\text{max}} = 726 \text{ nm}$  ( $\epsilon = 3.1 \text{ M}^{-1} \text{ cm}^{-1}$ ). These significant changes in the electronic spectrum suggest a binding mode of citrate in complex  $[\text{CoLH}_{-1}]^{2-}$ , similar in nature to the one mentioned above.

As stated previously, the pH-metric data could be equally well evaluated on the assumption of a dinuclear species  $[\text{Co}_2\text{L}_2\text{H}_{-2}]^{4-}$  (see model 1 in Table 4), being present in solution. This species is the dimeric form of  $[\text{CoLH}_{-1}]^{2-}$ . The proposed ligand-binding mode for such a dinuclear Co(II) species could probably be exemplified through a dihydroxo-bridged citrate complex. The alternative ligand-binding mode of bridging two  $[\text{CoLH}_{-1}]^{2-}$  units, with  $(\text{COO}^-, \text{O}^-, \text{COO}^-)$  coordination, through the other terminal  $\text{COO}^-$  moiety, forming a cyclic dimer, is not likely since the congener dinuclear species  $[\text{Co}_2\text{L}_2]^{2-}$  with a similar citrate binding mode, but with a protonated alcoholic OH, was not found in solution either. Furthermore, the dinuclear species through dihydroxo bridges is not an abundantly observed characteristic feature of Co(II) complexation in solution (in contrast to what is observed in the case of Cu(II), Al(III), or V<sup>IV</sup>O). We found a limited number of examples of purely dihydroxo-bridged dinuclear Co(II) systems in the literature.<sup>44</sup> Furthermore, no change in the intensity of the EPR spectra of the Co(II)–citric acid system in a 1:1 or 1:2 molar ratio was observed in frozen solutions. Thus, in the formation range of such a complex (a hydroxo-bridged dimer could contain antiferromagnetically coupled paramagnetic centers), the speciation model involving only mononuclear complexes seems to be much more probable. Unfortunately, the EPR features of the high-spin octahedral Co(II) complexes are rather complicated, because of the three unpaired electrons on the Co(II) and the significant zero field splitting, which can be comparable or even larger than the Zeeman effect. This is why the solution EPR measurements could be used only to monitor the concentration of the paramagnetic Co(II) centers and, in this way, assist in the exclusion of the formation of spin-paired dinuclear species.

(41) Kiss, E.; Kiss, T.; Jezowska-Bojczuk, M. *J. Coord. Chem.* **1996**, *40*, 157–166.

(42) Lakatos, A.; Bányai, I.; Bertani, R.; Decock, P.; Kiss, T. *Eur. J. Inorg. Chem.* **2001**, 461–469.

(43) Kiss, T.; Buglyo, P.; Sanna, D.; Micera, G.; Decock, P.; Dewaele, D. *Inorg. Chim. Acta* **1995**, *239*, 145–153.

(44) Hikichi, S.; Yoshizawa, M.; Sasakura, Y.; Akita, M.; Moro-oka, Y. *J. Am. Chem. Soc.* **1998**, *120*, 10567–10568.



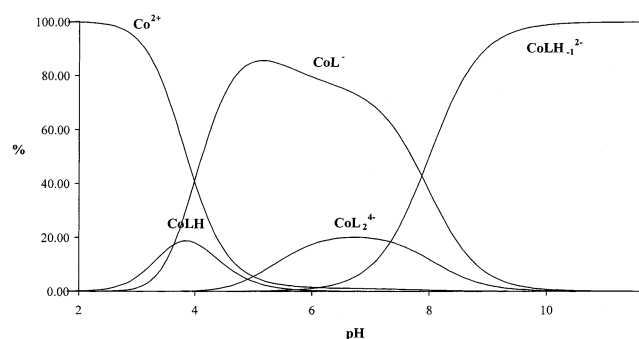


**Figure 6.** Speciation curves for the complexes formed in the Co(II)–citric acid system at 1:2 metal ion to ligand molar ratio and  $c_{\text{ligand}} = 0.004 \text{ M}$ .

It should be mentioned that, in the herein described speciation scheme, the resulting species are proposed to be octahedral, with the generated vacant coordination sites on each potential complex occupied by solvent water molecules. On the basis of such geometry around Co(II), coordination of tridentate and tetradentate citrates proceeds via both the central alcoholic and carboxylate groups as well as the terminal carboxylate moieties. This multipotent chemical diversity in the chemistry of citrate toward cobalt(II) has been observed before for other metal ions.<sup>45,46</sup> It reflects on the stability of the emerging metal–ligand complex, arising primarily from the formation of fairly stable five-membered ( $\text{CO}_2^-_{\text{central}}, \text{OH}_{\text{central}}$ ) and seven-membered ( $\text{CO}_2^-_{\text{central}}, \text{CO}_2^-_{\text{terminal}}$ ) metal chelate rings.

Overall, therefore, the binary Co(II)–citric acid system, as it is shown in the speciation curves depicted in Figure 6, can be well described by assuming the presence of a 1:1 complex  $[\text{CoLH}]^0$ , its deprotonated form  $[\text{CoL}]^-$ , the mononuclear species  $[\text{CoL}_2]^{4-}$ , and the fully deprotonated form  $[\text{CoLH}_{-1}]^{2-}$ . Of the purportedly potential species proposed in this investigation, the ones at high concentrations are (a)  $[\text{CoL}]^-$ , which appears to be 80% of the total species fraction in solution around  $\text{pH} \sim 6$ , and (b)  $[\text{CoLH}_{-1}]^{2-}$ , which appears to be 100% of the total species fraction in solution, at pH values greater than 10.

## Discussion

Facile aqueous reactions of Co(II) ion with the physiological ligand citric acid, at  $\text{pH} \sim 5$  with metal:ligand stoichiometries 1:1 and 1:2, led to the isolation of the first dinuclear  $[\text{Co}_2(\text{C}_6\text{H}_5\text{O}_7)_2(\text{H}_2\text{O})_4]^{2-}$  complex in the form of the potassium (**1**) and sodium (**2**) salts. Complexes **1** and **2**, however, were structurally different from the mononuclear complex  $[\text{Co}(\text{C}_6\text{H}_5\text{O}_7)_2]^{4-}$ , which was isolated with a ligand-to-metal ratio 1:2 and at higher pH values ( $\text{pH} \sim 7\text{--}8$ ).<sup>16</sup> Thus, the reactivity of the Co(II):citric acid system in aqueous solutions has shown that pH acts as a determining factor in the synthesis and isolation of different species of variable nuclearity and structural diversity.

With assessment of the structural features observed in both **1** and **2** as well as the complex  $[\text{Co}(\text{C}_6\text{H}_5\text{O}_7)_2]^{4-}$ , the

following observations are worth noting: (a) The Co(II) ions in all three complexes achieve a stable octahedral coordination, and (b) the central alcoholic group of the citrate ligand bound to Co(II) retains its proton in all three structures (in an equimolar solution and at  $\text{pH} > 8$ , however, the alcoholic OH may be deprotonated and may bind to Co(II) in the deprotonated form).

The major differences between the two classes of complexes, on the other hand, are: (a) the cobalt(II) ions employ different ligands ( $\text{C}_6\text{H}_5\text{O}_7^{3-}$ ,  $\text{H}_2\text{O}$ ) to satisfy their asymmetric octahedral environment in **1** and **2**, in contrast to complex  $[\text{Co}(\text{C}_6\text{H}_5\text{O}_7)_2]^{4-}$ , where the symmetric octahedral environment is shaped by the two citrate ligands ( $\text{C}_6\text{H}_5\text{O}_7^{3-}$ ), (b) the coordination ability of the terminal carboxylate group of the citrate ligand is different between complexes **1** and **2** and complex  $[\text{Co}(\text{C}_6\text{H}_5\text{O}_7)_2]^{4-}$ , (c) the nuclearity of complexes **1** and **2** (two) is different from that in complex  $[\text{Co}(\text{C}_6\text{H}_5\text{O}_7)_2]^{4-}$  (one), and (d) the charge on the dinuclear complexes **1** and **2** ( $2^-$ ) is lower than that in complex  $[\text{Co}(\text{C}_6\text{H}_5\text{O}_7)_2]^{4-}$  ( $4^-$ ).

The structural characteristics of the dinuclear complex anion in **1** emphasize the presence of a basic mononuclear unit in solution, which could be the scaffolding onto which the symmetric complex is assembled. Such an octahedral unit would contain a Co(II)-bound triply deprotonated citrate and three water molecules. Could, however, such a mononuclear complex exist in the solid state, or would the uncoordinated terminal  $\text{COO}^-$  function behave as a bridging group resulting in oligonuclear complex formation?

The magnetic susceptibility studies on complex **1** indicate the presence of two mononuclear Co(II) sites in the dimer, each with an effective ground-state  $S = 1/2$ , exhibiting a very small antiferromagnetic interaction. The presence of this weak exchange interaction is further suggested by magnetization studies and attested to by powder EPR studies on complex **1**. This result is not very surprising, in view of the fact that the two Co(II) ions are 5.247(1)–5.361(1) Å apart from each other. Therefore, both magnetics and EPR spectroscopy present a coherent picture of the magnetic character of the Co(II) ions in **1** in the solid state, strongly corroborating the presence of a dinuclear complex structure unraveled by X-ray crystallography.

Upon dissolution of complex **1** in water, however, the emerging EPR signal indicates the presence of a simple mononuclear octahedral Co(II) complex. The observed EPR signal is different from that of the dinuclear structure in the solid state and supports the idea of the dimer dissociating into its two constituent units. Corroborating to this end is the electronic spectrum of complex **1** in water, exhibiting absorption features similar to those previously observed for the well-characterized mononuclear complex  $[\text{Co}(\text{C}_6\text{H}_5\text{O}_7)_2]^{4-}$ , and the associated validity of the Lambert–Beer law over a wide concentration range (vide supra). It is conceivable, then, that when the monomer forms in the reaction solution, addition of the precipitating solvent or evaporation of the mother liquor leads to the solid-state structure of complex **1**.

What is the nature, however, of the monomer in solution? A detailed speciation study of the Co(II)–citrate aqueous

(45) Kiss, E.; Lakatos, A.; Banyai, I.; Kiss, T. *J. Inorg. Biochem.* **1998**, *68*, 145–151.

(46) Öhman, L.-O. *Inorg. Chem.* **1988**, *27*, 2565–2570.

system was carried out under varying Co(II) and citrate molar ratios throughout the pH range. Four major species arise from the derived speciation. One of them is a mononuclear octahedral species, the proposed formulation of which is  $[\text{Co}(\text{C}_6\text{H}_5\text{O}_7)]^-$ . Interestingly, the pH at which this species predominates is  $\sim 6$ , close to where the synthetic reactions are run leading ultimately to the isolation of the dinuclear complexes **1** and **2**. Being aware of the possibilities in the composition of the coordination environment around the Co(II) ion of this species in water, it would not be unreasonable to envisage an oxygen-based coordination sphere comprised of citrate carboxylate as well as bound water oxygens around Co(II). Likely, due to the relatively strong hydration of the complex, the bridging carboxylate functions in **1** are displaced by water molecules, and the dimer dissociates into the mononuclear complex  $[\text{CoL}]^-$ , bearing a  $(2\text{COO}^-, \text{OH}, 3\text{H}_2\text{O})$  coordination sphere. Thus, the speciation data on the mononuclear species are in line with the EPR and UV/visible spectroscopic data on complex **1** in solution. Both approaches unambiguously establish the presence of this species in the biodistribution scheme of Co(II) in aqueous citrate media.

A discrete species, also mononuclear, arisen at higher pH values ( $\sim 7$ – $8$ ) from the same speciation study, is the  $[\text{Co}(\text{C}_6\text{H}_5\text{O}_7)_2]^{4-}$  complex, for which ample evidence had been previously reported,<sup>16</sup> and is described in a comparative manner in this work. Here, too, speciation in association with tangible X-ray structural and spectroscopic data in the solid state and in solution have established concretely the presence of this well-defined species in a Co(II)–citrate distribution scheme.

At higher pH values ( $> 10$ ), new mono- or dinuclear species were proposed, contingent upon the deprotonation of either the bound citrate central  $\text{OH}_{\text{central}}$  or a water molecule in the coordination sphere of Co(II). Two model systems were put forward to account for the arisen ambiguity. Both of them provide sufficient chemical description of dinuclear complexes as potentially competent participants in the speciation of Co(II)–citrate system. Which species, however, is the actual species present at that high pH value awaits further synthetic efforts and constitutes a research challenge. At present, speciation and EPR results strongly suggest formation of the mononuclear complex  $[\text{CoLH}_{-1}]^{2-}$  in solution. In the low pH range the existence of a zero charge mononuclear species  $[\text{Co}(\text{C}_6\text{H}_6\text{O}_7)]^0$  is consistent with the double deprotonation of the citrate ligand at low pH.

Overall, the herein-developed chemistry suggests that, in the wide spectrum of pH-variable aqueous solutions, different species exist with variable solubility profiles, thus forging their isolation in the crystalline form, in the presence of specific counterions ( $\text{K}^+$ ,  $\text{Na}^+$ ,  $\text{NH}_4^+$ ). For two mononuclear species, of the four forms of Co(II)–citrate proposed in its aqueous speciation scheme, the solution behavior has been determined, and their physicochemical properties have been elucidated. Both  $[\text{Co}(\text{C}_6\text{H}_5\text{O}_7)]^-$  and  $[\text{Co}(\text{C}_6\text{H}_5\text{O}_7)_2]^{4-}$  complexes carry the electronic and structural signature of classical

Co(II) ions in aqueous media. These properties are significant attributes of Co(II), which bears in its coordination sphere a physiological ligand, citrate.<sup>47</sup> Hence, the  $[\text{Co}(\text{C}_6\text{H}_5\text{O}_7)]^-$  complex is another good example of a well-characterized species of potential biological relevance. Albeit optimally present at a pH value ( $\sim 5$ ) removed from the physiological pH,  $[\text{Co}(\text{C}_6\text{H}_5\text{O}_7)]^-$  may still play a key role in Co(II) processing and metabolic functions around the physiological pH, as it still exists as a component of the Co(II) speciation along with  $[\text{Co}(\text{C}_6\text{H}_5\text{O}_7)_2]^{4-}$  and  $[\text{CoLH}_{-1}]^{2-}$ . In this respect,  $[\text{Co}(\text{C}_6\text{H}_5\text{O}_7)]^-$  may reflect a form of Co(II) which is potentially capable of exerting, alone or in concert with the other species, influence on biochemical events relevant to (a) corrinoid biosynthesis or (b) toxic effects at the cellular level and aberrant physiological symptoms in human health.<sup>48–50</sup>

Finally, the herein characterized  $[\text{Co}(\text{C}_6\text{H}_5\text{O}_7)]^-$  complex and its solid-state dinuclear congener  $[\text{Co}_2(\text{C}_6\text{H}_5\text{O}_7)_2(\text{H}_2\text{O})_4]^{2-}$  reflect forms of Co(II), congruent with those previously proposed to exist,<sup>51,52</sup> which can be isolated and studied under variable experimental conditions contingent upon the physicochemical profiles of the solutions in which they are generated. In this context, species such as  $[\text{Co}(\text{C}_6\text{H}_6\text{O}_7)]^0$ ,  $[\text{CoLH}_{-1}]^{2-}$ , and others possibly yet unknown await careful perusal of their properties in solution and in the solid state. The structural speciation on the Co(II)–citrate system offers an example of how a systematic investigation, employing a multitude of techniques, can lead to the discovery and characterization of soluble, potentially bioavailable species of Co(II). Such species and their collective properties may help in the elucidation of the role that this metal ion plays at the biological level. To this end, pertinent research efforts are under way in our laboratories.

**Acknowledgment.** This work was supported with funds provided by the Department of Chemistry, University of Crete, Heraklion, Greece, and the National Science Research Fund (Grant OTKA 31896) and the Ministry of Education of Hungary (Grant FKFP 0013/97). The financial assistance to C.P.R. and A.T. by the Greek Secretariat of Athletics (OPAP) and Mrs. A. Athanassiou is gratefully acknowledged.

**Supporting Information Available:** X-ray crystallographic files, in CIF format, and listings of positional and thermal parameters and H-bond distances and angles and structure diagrams for  $(\text{Cat})_2[\text{Co}_2(\text{C}_6\text{H}_5\text{O}_7)_2(\text{H}_2\text{O})_4] \cdot 6\text{H}_2\text{O}$  (Cat =  $\text{K}^+$  (**1**),  $\text{Na}^+$  (**2**)). The material is available free of charge via Internet at <http://pubs.acs.org>.

IC011272L

(47) Martin, R. B. *J. Inorg. Biochem.* **1986**, *28*, 181–187.

(48) Kusaka, Y.; Jokohama, K.; Sera, Y.; Yamamoto, S.; Sone, S.; Kyono, H.; Shirakawa, T.; Goto, S. S. *Br. J. Int. Med.* **1986**, *43*, 474–485.

(49) Moorhouse, C. P.; Halliwell, B.; Grootveld, M.; Gutteridge, J. M. C. *Biochim. Biophys. Acta* **1985**, *843*, 261–268.

(50) Robison, S. H.; Cantoni, O.; Costa, M. *Carcinogenesis* **1982**, *3*, 657–662.

(51) Campi, E.; Ostacoli, G.; Meirone, M.; Saini, G. *J. Inorg. Nucl. Chem.* **1964**, *26*, 553–564.

(52) Li, N. C.; Lindenbaum, A.; White, J. M. *J. Inorg. Nucl. Chem.* **1959**, *12*, 122–128.